

Afterglow lightcurves, viewing angle and the jet structure of γ -ray bursts

Elena Rossi, Davide Lazzati & Martin J. Rees

Institute of Astronomy, University of Cambridge, Madingley Road, Cambridge CB3 0HA, England
e-mail: emr,lazzati,mjr@ast.cam.ac.uk

3 November 2018

ABSTRACT

Gamma ray bursts are often modelled as jet-like outflows directed towards the observer; the cone angle of the jet is then commonly inferred from the time at which there is a steepening in the power-law decay of the afterglow. We consider an alternative model in which the jet has a beam pattern where the luminosity per unit solid angle (and perhaps also the initial Lorentz factor) decreases smoothly away from the axis, rather than having a well-defined cone angle within which the flow is uniform. We show that the break in the afterglow light curve then occurs at a time that depends on the viewing angle. Instead of implying a range of intrinsically different jets – some very narrow, and others with similar power spread over a wider cone – the data on afterglow breaks could be consistent with a standardized jet, viewed from different angles. We discuss the implication of this model for the luminosity function.

Key words: Gamma-rays: bursts — X-rays: general — X-rays: ISM

1 INTRODUCTION

There are strong reasons for suspecting that the emitting plasma of γ -ray bursts (GRBs) is geometrically beamed in a cone. The energy requirements can then be reduced below the exorbitant levels that isotropic emission would imply (Kulkarni et al. 1999) and in most models for the long bursts it is in any case a natural expectation – borne out by simulations (MacFadyen & Woosley 1999; MacFadyen, Woosley & Heger 2001) – that the relativistic outflow from a central engine should be collimated along a channel that opens up along the rotation axis of a massive star. Although the relativistic MHD that gives rise to jets is uncertain, and surely very complicated, most discussions of the radiation from gamma ray bursts (and their afterglows) has postulated a jet with a well-defined angle (Meszaros & Rees 1997), though this angle may differ for different bursts (see, however, Meszaros, Rees & Wijers 1998; Salmonson 2001). We discuss here an alternative model where the jet, rather than having a uniform profile out to some definite cone angle, has a “beam pattern” where the power per unit solid angle (and perhaps also the initial Lorentz factor) is maximal along the axis, but drops off gradually away from the axis. This would be expected if there is mixing and entrainment from the borders of the funnel. We discuss the expected time-dependence of the afterglow if it is triggered by a jet with this more general profile. We conclude that the time of the observed break (which, for a uniform jet viewed along its axis, depends on the cone angle; see, e.g., Rhoads 1997) instead depends on the angle between the line of sight and the

symmetry axis: such a jet viewed nearly head-on simulates a narrow uniform jet, whereas the afterglow from the same jet viewed more obliquely would simulate a wider uniform jet. GRB have been proposed recently to be explosions releasing a standard power that can be either injected in very different jet opening angles or distributed within the jet in some universal emission diagram, (Postnov et al. 2001). While Frail et al. (2001, hereafter F01), support with their data the first interpretation, we show that their observational results could instead be attributed to a more standard set of objects viewed at different angles to their symmetry axis.

2 DYNAMICS AND BREAK TIME

We suppose that all long GRBs have jets with a standard opening angle θ_j , total kinetic energy and beam profile for $0 < \theta < \theta_j$. We consider a relativistic outflow where both the bulk Lorentz factor and the energy per unit solid angle depend as power laws¹ on the angular distance from the center θ

$$\epsilon = \begin{cases} \epsilon_c & 0 \leq \theta \leq \theta_c \\ \epsilon_c \left(\frac{\theta}{\theta_c}\right)^{-2} & \theta_c \leq \theta \leq \theta_j \end{cases} \quad (1)$$

and

¹ We concentrate here on a power index -2 motivated by F01 correlation. This is not, however, a necessary ingredient of the model as discussed in §6 (see also Fig. 3 and 4)

$$\Gamma = \begin{cases} \Gamma_c & 0 \leq \theta \leq \theta_c \\ \Gamma_c \left(\frac{\theta}{\theta_c}\right)^{-\alpha_\Gamma}, & \alpha_\Gamma > 0 \quad \theta_c \leq \theta \leq \theta_j, \end{cases} \quad (2)$$

where θ_c is introduced just for formal reasons to avoid a divergence at $\theta = 0$, but can be taken to be smaller than any other angle of interest. A lower limit to this angle is $\theta_c > 1/\Gamma_{\max} \sim 10^{-3}$ degrees, where $\Gamma_{\max} \sim 10^5$ is the maximum value to which the fireball can be accelerated (Piran 1999). The power law index of Γ , α_Γ , is not important for the dynamics of the fireball and the computation of the light curve as long as $\Gamma(t=0, \theta) \equiv \Gamma_0(\theta) > \theta^{-1}$ and $\Gamma_0(\theta) \gg 1, \forall \theta$. Nevertheless, it plays a role when we want to calculate the fraction of GRBs-afterglow without prompt γ -ray emission, as we discuss in §6.

Consider an observer at an angle $\theta_o < \theta_j$ with respect to the axis of the jet. He measures an isotropic equivalent energy $E_{iso} = 4\pi\epsilon(\theta_o)$ from the γ -ray fluence. If also the afterglow emission is dominated by the component pointing the earth, he will infer θ_o as the half-opening angle of the jet by means of the break time in the light curve, t_b (Sari, Piran & Halpern 1999) $\theta_j \propto t_b^{3/8} (E_{iso}/n)^{-1/8}$, where n is the external medium density. Since the total energy inferred from all viewing angles is $E_{tot} \simeq 2\pi\theta^2\epsilon = \text{const}$, the observer will derive the same conclusions obtained by F01 and Panaitescu & Kumar (2001, hereafter PK01) of GRBs as fireballs with the same total kinetic energy but very different jet apertures.

To evaluate how the contributions of the other components add to the light curve from the zone with $\theta \sim \theta_o$ we calculate when their beamed emission include the observer direction, (when $\theta - \theta_o < \frac{1}{\Gamma}$) and which energy per unit solid angle they have at that time compared to $\epsilon(\theta_o) \equiv \epsilon_o$. We show that under the assumptions of Eq. 1 the afterglow light curve is indeed dominated by the fireball element along the line of sight: neither the ‘‘core’’ of the jet with $\theta \ll \theta_o$ nor the regions with $\theta \gg \theta_o$ make substantial contributions.

For an effective though simplified discussion we consider only three components of the jet corresponding to $\theta = \theta_1 \ll \theta_o$, $\theta = \theta_o$ and $\theta = \theta_3 \gg \theta_o$. We call them ‘‘cone i ’’, where $i = 1, o, 3$, respectively. This approach is justified by the fact that only the very inner parts of the jet with $\epsilon \gg \epsilon_o$ and the much wider ($\pi\theta^2 \gg \pi\theta_o^2$) outer parts could contribute and substantially modify the light curve of cone o . We approximate cone 1 as a relativistic source moving at an angle θ_o with respect the observer, while the observer is approximately considered on the symmetry axis for cones o and 3. The cones, that are not causally connected ($\Gamma_0 > \theta^{-1}$), evolve independently and adiabatically in a constant density medium and spread sideways when Γ_i drops below θ_i^{-1} (Rhoads 1997). We consider relativistic lateral expansion of the cones so that their geometrical angles θ_i grow as $\theta_i \sim \theta_i(t=0) + \frac{t}{\Gamma_i}$. Since the dynamics of the fireball components changes at t_b , also Γ decreases with time differently before and after the break time. For $t < t_b$

$$\Gamma = \begin{cases} \Gamma_0 \left(\frac{t}{t_d}\right)^{-3/2} & \text{for } \theta_1 \\ \Gamma_0 \left(\frac{t}{t_d}\right)^{-3/8} & \text{for } \theta_o \text{ and } \theta_3, \end{cases} \quad (3)$$

where t_d is the deceleration time at which $\Gamma = \Gamma_0/2$ and the jet begins to decelerate significantly. From Eq. 3 to Eq. 8 we drop the subscript i for an easier reading. For $t > t_b$

$$\Gamma = \theta^{-1} \left(\frac{t}{t_b}\right)^{-1/2}. \quad (4)$$

This on-axis calculation is valid for all θ_i , because $\Gamma_1 \sim 1/\theta_o$ soon after the break time and the emitting plasma enters the line of sight: from this moment we can consider the observer to be on the cone axis. The lateral expansion starts at a time

$$t_b = \begin{cases} \theta^{2/3} \Gamma_0^{2/3} t_d & \text{for } \theta_1 \\ \theta^{8/3} \Gamma_0^{8/3} t_d & \text{for } \theta_o \text{ and } \theta_3, \end{cases} \quad (5)$$

where the deceleration time, t_d , depends on

$$t_d \propto \begin{cases} \epsilon^{1/3} \Gamma_0^{-2/3} (1 - \beta \cos \theta_o) & \text{for } \theta_1 \\ \epsilon^{1/3} \Gamma_0^{-8/3} & \text{for } \theta_o \text{ and } \theta_3, \end{cases} \quad (6)$$

and consequently

$$R_b \propto \theta^{2/3} \epsilon^{1/3}. \quad (7)$$

Therefore from Eq. 1 it follows that $R_b = \text{constant}$ and

$$t_b \propto \begin{cases} \theta^{2/3} \epsilon^{1/3} \theta_o^2 \propto \theta_o^2 & \text{for } \theta_1 \\ \theta^{8/3} \epsilon^{1/3} \propto \theta^2 & \text{for } \theta_o \text{ and } \theta_3. \end{cases} \quad (8)$$

Cones o and 3 are hollow but they spread only outwards because the inner components which have already expanded (for cone 3) or are about to do so (for cone o) have higher pressure. Eq. 8 shows also that when $\Gamma_1 \sim \theta_o^{-1}$ and the part of the blast generated by the core of the jet becomes visible to the observer, cone o has just started spreading. The contribution of region 1 to the light curve of the cone with θ_o is not dominant because when $\Gamma_1 \sim \theta_o^{-1}$ the energy per unit solid angle is comparable to ϵ_o

$$\epsilon_1 \simeq \epsilon_c \left(\frac{\theta_1}{\theta_c}\right)^{-2} \left(\frac{\pi\theta_1^2}{\pi\theta_o^2}\right) = \epsilon_o. \quad (9)$$

The regions with $\theta \gg \theta_o$ spread at later time, so when $\Gamma_3 \sim \theta_3^{-1}$ the energy per solid angle of cone o has already decreased with time but it remains always comparable to ϵ_3

$$\epsilon_o(t_{b3}) = \epsilon_o \theta_o^2 \Gamma_o^2(t_{b3}) = \epsilon_o \left(\frac{t_{b3}}{t_{b_o}}\right)^{-1} = \epsilon_o \left(\frac{\theta_3}{\theta_o}\right)^{-2} = \epsilon_3, \quad (10)$$

where t_{b_i} is the break time for cones i and we used Eq. 4 and Eq. 8.

Therefore the regions with $\theta \ll \theta_o$, (or those with θ substantially above θ_o), don't determine the overall shape of the light curve, because they are hidden by the dominant emission from the component along the line of sight. In principle, the superposition of many components of energy given by Eq. 9 and 10 may give rise to a sizable contribution. As shown by the more detailed calculation of § 3.2 (see Fig 2), this is not the case and the only effect is to delay by a factor of 2 the time of the break. Consequently the energy per unit solid angle that is measured modeling the afterglow is ϵ_o and the time break depends only on the viewing angle θ_o .

3 LIGHT CURVE CALCULATION

In order to compute a reasonably accurate lightcurve in our model, we adopt the following approach. We divide the inhomogeneous jet in N hollow cones (all but the very central one), each characterized by energy per unit solid angle and Lorentz factor given by Eq. 1. We compute an approximate lightcurve for each sub-jet using three asymptotic behaviors. For the cones with $\theta \lesssim \theta_o$ and $\theta \gtrsim \theta_o$ we adopt the $\theta \ll \theta_o$ and $\theta \gg \theta_o$ approximations described in § 2. For the cones

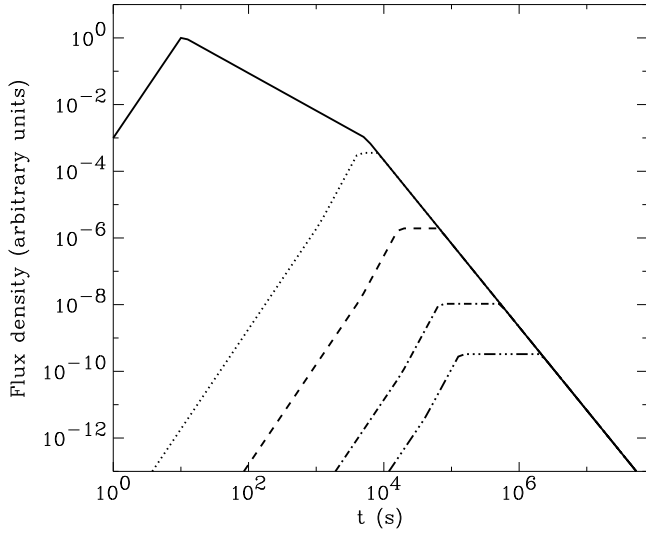


Figure 1. Light curves of an homogeneous jet (with uniform Γ and ϵ) as observed from different viewing angles. the geometric opening angle of the jet is $\theta_j = 1^\circ$. From top to bottom, with different line styles, off-axis angles $\theta_o = 0, 2, 4$ and 8 are shown.

defined by $\theta_o - 1/\Gamma < \theta < \theta_o + 1/\Gamma$ which point towards the observer since the beginning, we again consider the observer along the symmetry axis, but the emission is calculated in a filled cone geometry, instead of the hollow one adopted for the other cases. For $\theta > \theta_o - 1/\Gamma$ we use the usual afterglow theory to perform the lightcurve calculations, while for $\theta \lesssim \theta_o$ we generalize it for an off-axis observer as explained in the following section.

3.1 Radiation from an off-axis homogeneous fireball

Consider a uniform jet with Lorentz factor Γ and initial half-aperture θ_j . The radiative process is synchrotron emission (Meszaros & Rees 1997) and we concentrate on the power law branch of the spectrum between the peak, ν_m , and the cooling, ν_c , frequencies. The observed flux at a frequency ν , time t and viewing angle θ_o is

$$F(\nu, t, \theta_o) \propto A_e I' \left(\frac{\nu}{\delta}, \delta t \right) \delta^3(\Gamma, \theta_o), \quad (11)$$

where A_e is the emitting area and $\delta = (\Gamma(1 - \beta \cos \theta))^{-1}$ is the relativistic Doppler factor. I' is the comoving intensity at the comoving frequency $\nu' = \nu/\delta$ and at the comoving time $t' = \delta t$

$$I' = I'(\nu'_m, t') \left(\frac{\nu'}{\nu'_m} \right)^{-\alpha} \propto \Gamma^{(2+3\alpha)} \delta^{(1+\alpha)} t \nu^{-\alpha}. \quad (12)$$

Due to the relativistic beaming, the observed flux depends on the observer angle. In particular, if $\theta_o \simeq 0$

$$F = F_{on} \simeq \pi \left(\frac{R}{\Gamma} \right)^2 I' (2\Gamma)^3, \quad \forall t \quad (13)$$

while for $\theta_o > \theta_j$

$$F = F_{off} \simeq \begin{cases} \pi (R\theta)^2 I' \left(\frac{1}{\Gamma(1-\beta \cos \theta_o)} \right)^3 & t < t_b \\ \pi \left(\frac{R}{\Gamma} \right)^2 I' (2\Gamma)^3 & t > t_b. \end{cases} \quad (14)$$

In this case the jet is initially a source moving at an angle θ_o with the observer. At the break time $\Gamma \sim \theta^{-1}$ and then it

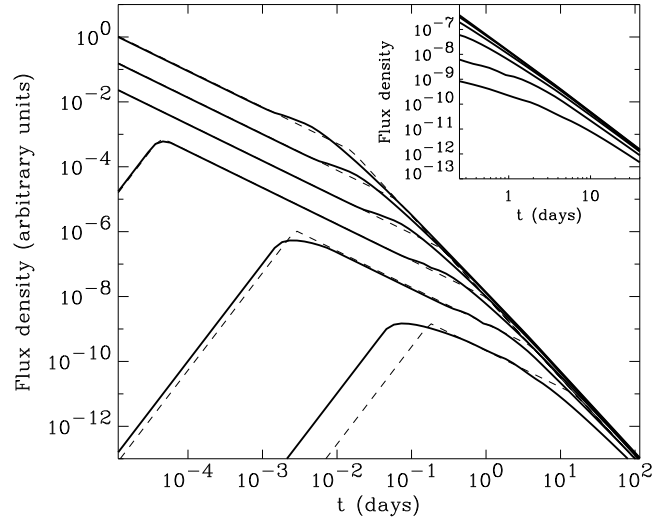


Figure 2. The light curves of an inhomogeneous jet observed from different angles. From the top we show $\theta_o = 0.5, 1, 2, 4, 8, 16^\circ$. The break time is related only to the observer angle: $t_b \propto \theta_o^2$. The dashed line is the on-axis light curve of an homogeneous jet with an opening angle $2\theta_o$ and an energy per unit solid angle $\epsilon(\theta_o)$. The blow up is the time range between 4 hours and 1 month, where most of the optical observations are performed. Comparing the solid and the dashed lines for a fixed θ_o , it is apparent that we can hardly distinguish the two models by fitting the afterglow data. The slight flattening of the lightcurves just before the break is likely to be due to the numerical approximations we adopted (see § 3).

starts decreasing very fast (Eq. 3) until $\theta_o - \theta_j < \frac{1}{\Gamma}$ and we can again use the approximation that the jet is viewed on-axis. So the intensity, the change in the slope and the break time of the afterglow depend on the observer viewing angle. In Fig. 1 we show the resulting off-axis lightcurve for a jet with opening angle $\theta_j = 1^\circ$ as viewed with off-axis angles $\theta_o = 0, 2, 4$ and 8 degrees. The flat part of the lightcurves corresponds to the time interval between the beginning of the jet spreading and the time in which the jet enters the line of sight. In this time interval our approximations are no longer valid and we simply model the lightcurve with a flat component connecting earlier and later times. This crude approximations is likely responsible for the slight flattening of the final lightcurves (see below and Fig. 2) just before the break.

3.2 Inhomogeneous jet

Using Eq. 13 and Eq. 14 we can compute the total light curve as a sum over the fireball components according to the scheme described at the beginning of this section.

$$L(\nu, t, \theta_o) = \sum_{\theta < \theta_o - \frac{1}{\Gamma}} \left[F_{off} \left(\frac{\theta^2 - \theta_{in}^2}{\theta^2} \right) \right] + \sum_{\theta_o - \frac{1}{\Gamma} < \theta < \theta_o + \frac{1}{\Gamma}} \left[F_{on} \frac{1}{N} \right] + \sum_{\theta > \theta_o + \frac{1}{\Gamma}} \left[F_{on} - F_{on}(\theta_{in}) \right], \quad (15)$$

where θ_{in} is the inner edge of the cone and $F_{on}(\theta_{in})$ is the light curve for a jet with $\epsilon(\theta)$, $\Gamma(\theta)$ and half-opening angle θ_{in} . N is the number of jet components that are beamed around the line of sight at small times.

The results of this calculation are shown in Fig. 2 for different viewing angles. On top of the solid lines we plot with a dashed line the lightcurve of a homogeneous fireball with $\epsilon = \epsilon_o$ and $\theta_j = \theta_o$. This shows that, for $\theta_o < \theta_j$, the lightcurve of an inhomogeneous jet can be successfully modelled with the lightcurve expected for a homogeneous jet: $F \propto t^{-3(p-1)/4}$ for $t < t_b$ and $F \propto t^{-p}$ for $t > t_b$.

One of the main simplifications that we made in Eq. 15 is to assume that the observer is on the jet axis of the cones with $\theta \geq \theta_o$. The main consequence is to predict a transition between the two power-law branches sharper than what we expect from the exact integration. This is due to the fact that, even in a uniform jet, off-axis observers sees smoother transitions (see Fig. 4 of Ghisellini & Lazzati 1999).

4 TIME BREAK-ENERGY RELATION

Recently an important observational result on the energetic content of GRBs was published by PK01 and F01. They found an anti-correlation between the isotropic equivalent energy, $E_{iso} = 4\pi\epsilon$ and the break time in the afterglow lightcurves. F01 in particular derived E_{iso} from gamma ray fluences, $F_\gamma \propto E_{iso}$ and their data are consistent with $F_\gamma \propto t_b^{-1}$. They explain it in the framework of collimated, uniform, lateral spreading jets interacting with a constant, low density (0.1 cm^{-3}), external medium. The observer is postulated to be along the jet axis. They assume that the afterglow emission steepens because at that time the Lorentz factor has dropped to $\Gamma \sim \theta_j^{-1}$, so that the on-axis observer sees the edge of the jet and the lateral jet spreading becomes important. In this case $E_{iso} \propto t^{-1}$ is predicted, which matches observation. They convert the observed break times in jet opening angles through the formulation of Sari et al. (1999). The γ -ray energy measured and corrected for the inferred geometry of the jet is clustered around 5×10^{50} erg. They concluded that GRBs central engines release the same amount of energy through jets with very different opening angles. In this framework, then, the wide distributions in kinetic energy per unit solid angle, which spans 3 orders of magnitude, is due only to the distribution of jet solid angles. PK01 obtained the same results, modeling a subset of multiwavelength afterglows from which they could assign an external density, a time break and an equivalent isotropic energy for the fireball. Both F01 and PK01 found geometric angles that span an order of magnitude but strongly concentrate around $2^\circ - 4^\circ$. In the framework of our model an alternative explanation of the observed relation between E_{iso} and t_b can be found. As discussed in §2 and shown in Fig. 2, we can infer from observations only the properties of the cone pointing towards the observer and not those of the whole jet. So $E_{iso} = 4\pi\epsilon_o$ and using Eq. 8 and Eq. 1 we obtain

$$E_{iso} \propto \theta_o^{-2} \propto t_b^{-1}. \quad (16)$$

Then, the observed distribution of E_{iso} and its relation with t_b is due to an inhomogeneous jet and the possibility to view it from different angles.

5 LUMINOSITY FUNCTION

Under our assumptions, each γ -ray luminosity corresponds to a particular viewing angle. The probability to see a jet between θ and $\theta + d\theta$ is given by

$$P(\theta)d\theta \propto \sin \theta d\theta \quad 0 \leq \theta \leq \theta_j, \quad (17)$$

$\langle \theta \rangle \simeq 0.7$ and the highest probability is for $\theta = \theta_j$. Therefore it is highly improbable to see a jet on axis. Consequently we expect more faint GRBs than very luminous ones according to a luminosity function

$$P(y) \propto 10^{-y}, \quad (18)$$

where $y = \log \epsilon$.

Since there are only a small number of GRBs with observed red-shift, the comparison of our predicted luminosity function with data is far from being definitive. Recently Bloom et al. (2001) published an histogram of the bolometric k-corrected prompt energies for 17 GRBs. The distribution is roughly flat from 6×10^{51} to 2×10^{54} erg but as the authors emphasize this analysis applies only to observed GRBs with redshifts and several observational biases obscure the true underlying energy distribution. The main bias that overcasts faint GRBs is the detection threshold of the instruments: this sample is thus flux and not volume limited. Moreover redshift determination encounters more problem for faint GRBs. Based on $\langle V/V_{max} \rangle$ -hardness correlation, Schmidt (2001) derived a luminosity function without using any redshift. They had to assume how the comoving GRBs rate varies with redshift and they based their calculations on three star forming rate models. In this case a power-law luminosity function was derived, but flatter than the $n(L) \propto L^{-2}$ predicted in the simplest version of our model. A luminosity function not based on assumed burst rate evolution can be derived by measuring the burst distance scale through the recently discovered variability-luminosity relation (Fenimore & Ramirez-Ruiz 2000, Reichart et al. 2001). A cumulative analysis of a sample of 220 bursts (Fenimore & Ramirez-Ruiz 2000) yielded a power-law luminosity function $n(L) \propto L^{-2.33}$, which compare more favorably with our prediction. More recently, Lloyd-Ronning, Fryer & Ramirez-Ruiz (2001) find that the typical luminosity of GRBs evolves with redshift. As a consequence, a flatter power-law index $n(L) \propto L^{-2.2}$ is obtained. We stress, however, that our deduced luminosity function can be altered by distributions in total energy or geometric angles or by luminosity evolution with redshift. Given the somewhat contradictory observational results discussed above, we conclude that more accurate spectral and fluence measures and a larger sample of bursts are needed for a proper comparison.

6 DISCUSSION AND CONCLUSIONS

We considered inhomogeneous GRBs jets with a standard total energy, opening angle and local energy distribution, $\epsilon \propto \theta^{-2}$. We show that this jet structure can reproduce the observed correlation between isotropic energy and break-time. In this model both measurements depend only on the viewing angle because the γ -ray fluence and the afterglow emission are dominated by the components of the jet pointing towards the observer at small times. Since all cones have

the same total energy $E_{\text{jet}} = 2\pi\theta^2\epsilon = \text{const}$, we recover the results of F01 and PK01 but the constraints on the geometrical beaming can be relaxed and an appealing more standard structure for all GRBs can be adopted. The jet total energy can be calculated from Eq. 1

$$E_{T\text{total}} = 2\pi\epsilon_c\theta_c^2 \left(1 + 2\ln\frac{\theta_j}{\theta_c}\right) = E_{\text{jet}} \left(1 + 2\ln\frac{\theta_j}{\theta_c}\right) \quad (19)$$

and compared to $E_{\text{jet}} = 2\pi\theta_o\epsilon_o = 2\pi\epsilon_c\theta_c^2$, the total energy inferred from observation, $E_{\text{jet}} \leq E_{T\text{total}}$. To give an example, for a fireball with $\theta_c = 1^\circ$ and $\theta_j = 20^\circ$, we have $E_{T\text{total}}/E_{\text{jet}} \simeq 6$, i.e. the true energy of the fireball can be one order of magnitude larger than what inferred with the models of F01 and PK01.

In addition (§ 5) we can derive the GRBs luminosity function from the probability distribution of the viewing angle and compare it to data. The comparison is, at this stage, still uncertain because more accurate spectral and fluence measures are required to build a volume limited sample and confirm (or rule out) this model.

In any fireball model considering a jet-like GRB structure, a certain number of afterglows without γ -ray emission (orphan afterglows) is expected. For an homogeneous jet, orphan afterglows are possible only for viewing angles greater than $\theta_j + 1/\Gamma$. In our jet configuration a fraction of the total area could have a Lorentz factor lower than the minimum Γ necessary for γ -ray radiation. Consequently, considering the same opening angle, an inhomogeneous jet could produce an higher fraction of orphan afterglows than an homogeneous one. This intrinsic fraction depends above all on the Γ distribution within the jet (α_Γ in Eq 2) and on the minimum Lorentz factors to produce γ -ray radiation and afterglow emission. The observed number of orphan afterglows depends also on flux detection limits, GRB explosion rates with redshift and cosmology. An accurate calculation of the expected orphan afterglow rates is therefore beyond the scope of this paper.

We emphasize that we implicitly assumed the radiation efficiency of the fireball to be weakly dependent on Γ or ϵ . This is a plausible assumption in internal-shocks scenario. If it was not the case and the efficiency grew with ϵ , a different relation between ϵ and θ should be postulated in order to reproduced observations. In this paper we concentrated for simplicity on a beam profile $\epsilon \propto \theta^{-2}$ which is consistent observational results but it is interesting to briefly discuss other power-law relations $\epsilon \propto \theta^{-\alpha_\epsilon}$ (see Fig. 3). A decay flatter than 2 would cause two breaks in the light curve: the first due to the cone pointing the observer when $\Gamma(\theta_o) \sim \theta_o^{-1}$ and the second, at later times, when the observer sees the edge of the jet and $\Gamma(\theta_j) \sim \theta_j^{-1}$. The power law index after the first break is flatter then t^{-p} because the cones with $\theta_o < \theta \leq \theta_j$ enter the line of sight with $\epsilon \geq \epsilon_o$ and substantially modify the light curve shape. With a steeper decay in the distribution of ϵ the time break and the emission after that break would be dominated by the jet along the axis rather than by the very much weaker part directed to the observer. The jet break would then be preceded by a prominent flattening in the lightcurve, especially for $\alpha_\epsilon > 3$, difficult to reconcile with observations. In this case we would have γ -ray emission only for very small angles and the number of orphan afterglows would be much greater then expected from the $\alpha_\epsilon = 2$ model. From Eq. 8 we can derive

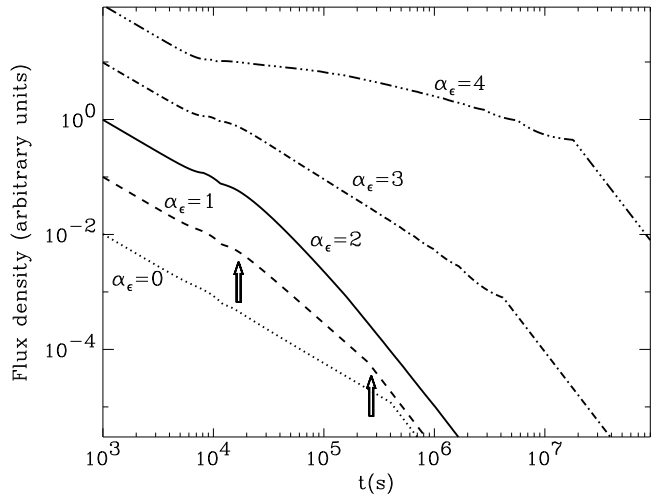


Figure 3. The lightcurves of inhomogeneous jets with different indices α_ϵ ($\epsilon \propto \theta^{-\alpha_\epsilon}$). The lightcurves have the same ϵ_o but they are plotted shifted by factors of 10 for clarity (they would be indistinguishable at small time). The arrows highlight the location of the two breaks for $0 < \alpha < 2$.

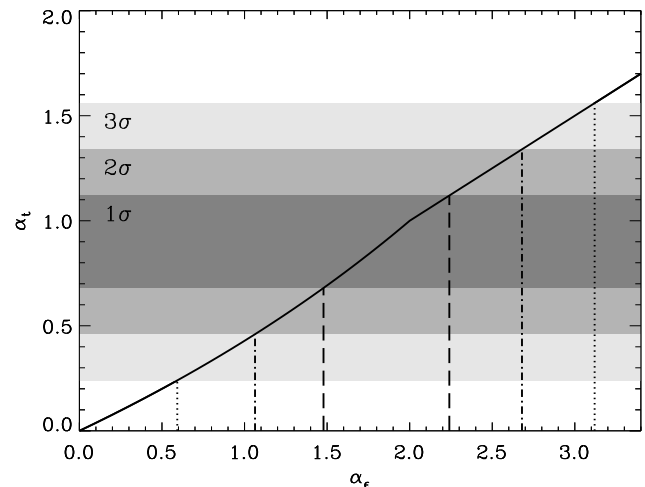


Figure 4. The relation between the indices α_t ($E_{\text{iso}} \propto t_b^{-\alpha_t}$) and α_ϵ ($\epsilon \propto \theta^{-\alpha_\epsilon}$) from an inhomogeneous jet. The shaded regions show the best fit to F01 data $\alpha_t = 0.9 \pm 0.22$.

the relation between the index α_ϵ and α_t (where $E_{\text{iso}} \propto t_b^{\alpha_t}$). We obtain $\alpha_t = \alpha_\epsilon/2$ for $\alpha_\epsilon \geq 2$ and $\alpha_t = 3\alpha_\epsilon/(8 - \alpha_\epsilon)$ for $\alpha_\epsilon < 2$, when the first break is considered. In Fig. 4 we plot this relation overlaid on the interval in α_t allowed by observations (we used F01 data). We derive $1.5 \lesssim \alpha_\epsilon \lesssim 2.2$, at the 1σ level. Further γ -ray and afterglow observations will allow to constrain this parameter much better in the future.

Besides the luminosity function discussed in § 5, there are several ways in which this model can be proved or disproved. First, we have shown that the real total energy of the fireball can easily be an order of magnitude larger than what estimated by PK01 and F01. In this case, after the fireball has slowed down to mild-relativistic and sub-relativistic speed, radio calorimetry (Frail, Waxman & Kulkarni 2000) should allow us to detect the excess energy. In addition, in this model we naturally predict that the more luminous part of the fireball have higher Lorentz factors. This may help

explaining the detected luminosity-variability (Fenimore & Ramirez-Ruiz 2000) and luminosity-lag (Norris, Marani & Bonnell 2000) correlations (Salmonson 2000, Kobayashi, Ryde & MacFadyen 2001; Ramirez-Ruiz & Lloyd-Ronning 2002). Another constrain is given by polarization. Since fire-ball anisotropy is a basic ingredient of this model, inducing polarization (Ghisellini & Lazzati 1999; see also Sari 1999 and Gruzinov & Waxman 1999). The time evolution of the polarized fraction and of the position angle are however different from a uniform jet (Rossi et al. in preparation). Finally, the properties of the bursts should not depend on the location of the progenitor in the host galaxy, and therefore this model can accommodate the marginal detection of an E_{iso} -offset relation (Ramirez-Ruiz, Lazzati & Blain 2001) only if a distribution of θ_j is considered.

ACKNOWLEDGMENTS

We thank G. Ghisellini, J. Granot, P. Kumar, A. Panaitescu and E. Ramirez-Ruiz for many stimulating discussions. ER and DL thank the IAS, Princeton, for the kind hospitality during the final part of the preparation of this work. ER thanks the Isaac Newton and PPARC for financial support.

REFERENCES

- Bloom J. S., Frail D. A., Sari R., 2001, *AJ*, 121, 2879
 Fenimore E. E., Ramirez-Ruiz E., 2000, *ApJ* submitted (astro-ph/0004176)
 Frail D. A., Waxman E., Kulkarni S. R., 2000, *ApJ*, 537, 191
 Frail D. A., et al., 2001, *ApJ*, 562, L55
 Ghisellini G., Lazzati D., 1999, *MNRAS*, 309, L7
 Gruzinov A., Waxman E., 1999, *ApJ*, 511, 852
 Kobayashi S., Ryde F., MacFadyen A., *ApJ* submitted (astro-ph/0110080)
 Kulkarni S. R., et al., 1999, *Nature*, 398, 389
 Lloyd-Ronning N. M., Fryer C. L., Ramirez-Ruiz E., 2001, *ApJ*, in press (astro-ph/0108200)
 MacFadyen A. I., Woosley S. E., 1999, *ApJ*, 524, 262
 MacFadyen A. I., Woosley S. E., Heger A., 2001, *ApJ*, 550, 410
 Meszaros P., Rees M. J., 1997, *ApJ*, 476, 232
 Meszaros P., Rees M. J., Wijers R. A. M. J., 1998, *ApJ*, 499, 301
 Norris J. P., Marani G. F., Bonnell J. T., 2000, *ApJ*, 534, 248
 Panaitescu A., Kumar P., 2001, 560, L49
 Piran T., 1999, *Physics Rep.*, 314, 575
 Postnov K. A., Prokhorov M. E., Lipunov V. M., 2001, *Astronomy Report*, 45, 236
 Ramirez-Ruiz E., Lazzati D., Blain A. W., 2002, *ApJ*, 565, L9
 Reichart D. E., Lamb D. Q., Fenimore E. E., Ramirez-Ruiz E., Cline T. L., Hurley K., 2001, *ApJ*, 552, 57
 Rhoads J. E., 1997, *ApJ*, 487, L1
 Salmonson J. D., 2000, *ApJ*, 544, L115
 Salmonson J. D., 2001, *ApJ*, 546, L29
 Sari R., 1999, *ApJ*, 524, L43
 Sari R., Piran T., Halpern J. P., 1999, *ApJ*, 519, L17
 Schmidt M., 2001, *ApJ*, 552, 36